AIP ADVANCES 6, 065308 (2016)

Graphene-based Yagi-Uda antenna with reconfigurable radiation patterns

Yongle Wu,[1,a,b] Meijun Qu,[1,a] Lingxiao Jiao,[1] Yuanan Liu,[1] and Zabih Ghassemlooy[2]
[1]*School of Electronic Engineering, Beijing Key Laboratory of Work Safety Intelligent Monitoring, Beijing University of Posts and Telecommunications, P. O. Box. 282, Beijing, 100876, China*
[2]*Optical Communications Research Group, NCRLab, Faculty of Engineering and Environment, Northumbria University, Newcastle upon Tyne, NE1 8ST, U.K.*

(Received 6 February 2016; accepted 2 June 2016; published online 9 June 2016)

This paper presents a radiation pattern reconfigurable Yagi-Uda antenna based on graphene operating at terahertz frequencies. The antenna can be reconfigured to change the main beam pattern into two or four different radiation directions. The proposed antenna consists of a driven dipole radiation conductor, parasitic strips and embedded graphene. The hybrid graphene-metal implementation enables the antenna to have dynamic surface conductivity, which can be tuned by changing the chemical potentials. Therefore, the main beam direction, the resonance frequency, and the front-to-back ratio of the proposed antenna can be controlled by tuning the chemical potentials of the graphene embedded in different positions. The proposed two-beam reconfigurable Yagi-Uda antenna can achieve excellent unidirectional symmetrical radiation pattern with the front-to-back ratio of 11.9 dB and the10-dB impedance bandwidth of 15%. The different radiation directivity of the two-beam reconfigurable antenna can be achieved by controlling the chemical potentials of the graphene embedded in the parasitic stubs. The achievable peak gain of the proposed two-beam reconfigurable antenna is about 7.8 dB. Furthermore, we propose a four-beam reconfigurable Yagi-Uda antenna, which has stable reflection-coefficient performance although four main beams in reconfigurable cases point to four totally different directions. The corresponding peak gain, front-to-back ratio, and 10-dB impedance bandwidth of the four-beam reconfigurable antenna are about 6.4 dB, 12 dB, and 10%, respectively. Therefore, this novel design method of reconfigurable antennas is extremely promising for beam-scanning in terahertz and mid-infrared plasmonic devices and systems. [http://dx.doi.org/10.1063/1.4953916]

I. INTRODUCTION

It is observed that the graphene technology has attracted growing interests and its potential applications for various fields have been discovered in the last decade. The gapless energy spectrum in graphene makes it an attractive candidate for massive nan-oelectronics and nan-ophotonics devices[1–3] such as terahertz antennas,[4–6] filters,[7,8] oscillators,[9] plasmonic Bragg reflectors,[10] absorbers,[11] and surface acoustic-wave amplifiers.[12] Since the surface complex conductivity of graphene can be dynamically controlled by changing the applied voltage, it opens up unprecedented opportunities in developing reconfigurable plasmonic devices at terahertz and mid-infrared frequencies.

[a]Yongle Wu and Meijun Qu contributed equally to this work.
[b]wuyongle138@gmail.com.

The Yagi-Uda antenna is a typical end-fire antenna composed of the radiation and parasitic elements, which has been widely adopted for TV signal reception. It is fed by only a single feeding port, and the parasitic element is excited by means of electromagnetic coupling of the dipole antenna. Besides the simple structure, Yagi-Uda antennas have the potential to be designed as pattern reconfigurable antennas[13–16] covering the full azimuth plane. The classical reconfigurable Yagi-Uda antennas are designed by switching the state of PIN diodes inserted on parasitic elements, forcing them to act as directors or reflectors and thus changing the main beam direction. However, the conventional electronic based control switches are not available in the terahertz frequency range due to the limited frequency performance. Fortunately, graphene can be introduced as the "switch" for terahertz-frequency devices because of its active complex conductivity. Some antennas take advantage of the graphene by making the frequency or the radiation pattern reconfigurable[17–23] such as the MIMO antennas,[17] leaky-wave antennas,[18,19] Yagi antennas,[20] microstrip quasi-Yagi antennas,[21] reflect-array antennas,[22] slot antennas,[23] and dipole antennas.[24,25] The antennas proposed in Refs. 17–22 have reconfigurable dynamic radiation patterns, but the beam adjustable range is limited.

In this paper, a type of graphene-based reconfigurable Yagi-Uda antenna with two or four radiation patterns is proposed, where the radiation patterns can cover the full azimuth plane. The direction of main radiation beam is controlled by different chemical potentials applied on the parasitic stubs' graphene. We show that the variable chemical potential could affect the front-to-back ratio and the resonance frequency of the proposed antenna. Furthermore, we outline that the proposed reconfigurable antenna is valid for graphene-based Yagi-Uda antennas with more radiation patterns (i.e., 6-, 8- patterns and so on). Such antennas with high directionality (i.e., high gain) could be ideal for a number of applications including wireless sensor networks,[26] and the last mile access network employing hybrid free space optics and radio frequency technologies,[27] which offer improved link performance. Due to the advancement of the planar implementations, the graphene-metal hybrid implementation in Refs. 19 and 28–30 has become available. In particular, this technology has been demonstrated experimentally in Ref. 30.

The rest of the paper is organized as follow. The following sections describe the antenna configuration and radiation mechanism based on the graphene. Section II provides a two-beam pattern reconfigurable Yagi-Uda antenna. Section III proposes a Yagi-Uda antenna with four reconfigurable beams by extending the design method outlined in Section II. Finally the concluding remarks are presented in Section IV.

II. THE DESIGN OF A TWO-BEAM RECONFIGURABLE YAGI-UDA ANTENNA

The reconfigurable terahertz graphene-based Yagi-Uda antenna with two-beam patterns is simulated using the Full-Wave Electromagnetic Simulator. Graphene with a single atom thickness can be modeled as a 2-D surface with complex conductivity σ. The conductivity is composed of two elements: the inter-band and intra-band as defined by Kubo's formulas[31–33]

$$\sigma_{\text{intra}} \approx \frac{-je^2 k_B T}{\pi\hbar^2(\omega - j2\Gamma)}\left[\frac{\mu_c}{k_B T} + 2\ln\left(e^{-\mu_c/(k_B T)} + 1\right)\right], \tag{1}$$

$$\sigma_{\text{inter}} \approx \frac{-je^2}{4\pi\hbar}\ln\left(\frac{2|\mu_c| - (\omega - j2\Gamma)\hbar}{2|\mu_c| + (\omega - j2\Gamma)\hbar}\right), \tag{2}$$

where e is the electron charge, ω is the angular frequency, k_B is the Boltzmann constant, $\hbar$ is the reduced Plank constant, T is the temperature in Kelvin, τ is the electron relaxation time, and $\Gamma = 1/(2\tau)$ is the electron scattering rate. Here assuming $T = 300$ K and $\tau = 1$ps, which is similar with the condition in Ref. 34, and only the intra-band contribution is considered in this study. The used substrate is constructed by SiO_2 with a dielectric constant of 3.8 and a thickness of 1μm. In addition, μ_c represents the chemical potential applied to the graphene stubs.

Figure 1 presents the layout schematic of the two-beam reconfigurable Yagi-Uda antenna with the geometrical parameters. It consists of a driven dipole radiation conductor (fed by a 50 Ω source) and two parasitic elements. Both parasitic elements are integrated with graphene (shown as black

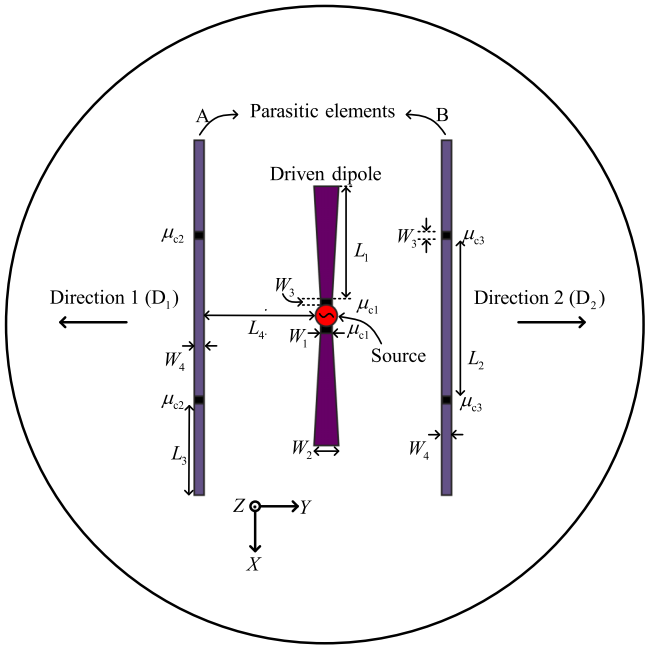

FIG. 1. Configuration of the two-beam pattern reconfigurable Yagi-Uda antenna with geometrical parameters.

dots) and are supplied with different chemical potentials to control the radiation direction. The graphene strips implanted in the dipole antenna are used for connecting the two radiation arms, with the applied chemical potential μ_{c1} of 0.4 eV. If the chemical potential μ_{c2} is set to 0.4 eV and μ_{c3} is set to 0 eV, the corresponding parasitic elements A and B in Figure 1 behave as a director and a reflector for the –Y direction 1 (D_1), respectively. Similarly, when the chemical potential μ_{c2} is set to 0 eV and μ_{c3} is set to 0.4 eV, the corresponding parasitic elements A and B in Figure 1 perform as a reflector and a director for the +Y direction 2 (D_2), respectively. This is because the conductivity could be alternated by integrating graphene strips. Based on this property a reconfigurable two-beam Yagi-Uda antenna is proposed. All the accurate values of geometrical parameters are listed in TABLE I.

Figure 2 shows the current distributions for the proposed antenna for D_1 and D_2 with identical excitation signals. In Figure 2(a) with the chemical potentials μ_{c2} of 0.4 eV and μ_{c3} of 0 eV, the left (A) and right (B) parasitic strips acts as a director and a reflector, respectively. Since the left parasitic strip (A) is inductive, the phase of the current in parasitic element lags the dipole radiation element's current.[35] The current distribution changes when the μ_{c2} and μ_{c3} are set to 0 eV and 0.4 eV, respectively. In this case, the right (B) and left (A) parasitic strips act as a director and a reflector, respectively as shown in Figure 2(b). Because of the graphene with a complex conductivity, the conductivity of the parasitic elements can be altered by simply controlling the chemical potentials μ_{c2} and μ_{c3}. Figures 3(a) and 3(b) illustrate the simulated radiation patterns of the proposed two-beam reconfigurable Yagi-Uda antenna at 3.73 THz for both D_1 and D_2 in the *XOY* and *YOZ* Planes. Excellent unidirectional symmetrical radiation patterns with the 11.9 dB front-to-back ratio have been achieved by simply alerting the chemical potentials μ_{c2} and μ_{c3}. The achievable

TABLE I. The geometrical dimensions of the proposed two-beam reconfigurable Yagi-Uda antenna.

Parameters	Value (μm)	Parameters	Value (μm)	Parameters	Value (μm)
W_1	2	W_2	6	W_3	1.6
W_4	2	L_1	22	L_2	28.4
L_3	21.2	L_4	14.9		

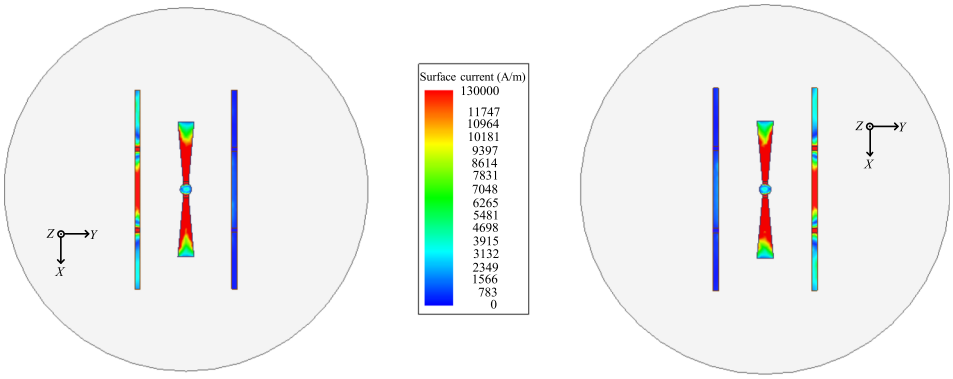

(a) (b)

FIG. 2. Current distributions for the proposed two-beam reconfigurable Yagi-Uda antenna at 3.73 THz: (a) D_1, $\mu_{c2} = 0.4$ eV, and $\mu_{c3} = 0$ eV, and (b) D_2, $\mu_{c2} = 0$ eV, and $\mu_{c3} = 0.4$ eV.

gain of this proposed antenna is about 7.8 dB. Figure 4 depicts the simulated reflection coefficients $|S_{11}|$ for both D_1 and D_2, for this proposed antenna. Note that the reflection coefficients are highly stable in both two radiation directions D_1 and D_2. It can be observed in Figure 4 that this antenna is resonating at 3.73 THz and the 10-dB impedance bandwidth is about 15%.

As can be seen from Figures 5 and 6, the chemical potential μ_{c3} for D_2 does affect the front-to-back ratio and the resonating frequency position of the proposed antenna, simultaneously. Figures 5(a) and 5(b) show the simulated radiation patterns (*XOY* and *YOZ* planes) of the proposed antenna for D_2 ($\mu_{c1} = 0.4$ eV and $\mu_{c2} = 0$ eV) with the chemical potential μ_{c3} of 0.4 eV, 0.6 eV, and 0.8 eV applied to the right (B) parasitic strips at 3.73 THz. The right (B) graphene-based director guides the radiation toward the +Y direction. The front-to-back ratios are radically changed from 11.9 dB to 6.7 dB when the chemical potential μ_{c3} varies from 0.4 eV to 0.8 eV. Figure 6 plots the corresponding reflection coefficients $|S_{11}|$ as a function of frequency for these three values of μ_{c3}. The reflection-coefficient results show that the chemical potential μ_{c3} can affect impedance-matching performance. In order to further clarify the values of chemical potentials for two directions (D_1 and D_2), TABLE II depicts the corresponding values of the chemical potentials for two directions (D_1 and D_2) in the proposed antenna with two reconfigurable beams.

The effect of relaxation time τ on the performance of the proposed two-beam reconfigurable Yagi-Uda antenna is discussed here. It can be seen clearly from Figure 7 that the performance variations for different electron relaxation time τ are very small. In Figure 7(a), the resonance frequency varies from 3.63 THz to 3.73 THz when the electron relaxation time τ changes from 0.2 ps to 1.0 ps.

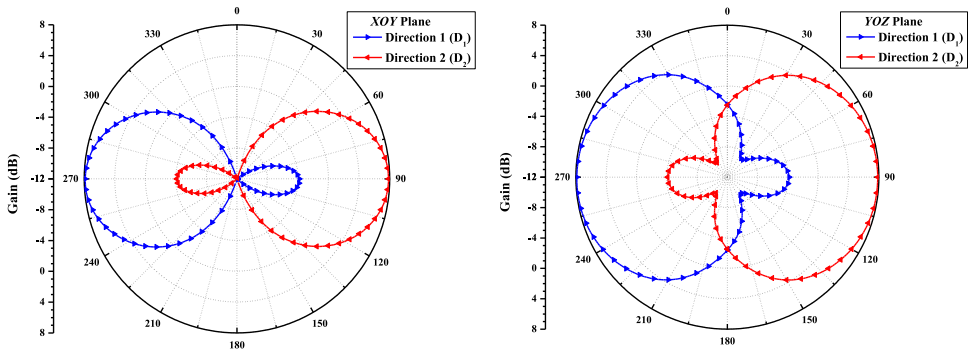

(a) (b)

FIG. 3. Simulated radiation patterns for the two-beam reconfigurable Yagi-Uda antenna at 3.73 THz: (a) *XOY* Plane, and (b) *YOZ* Plane.

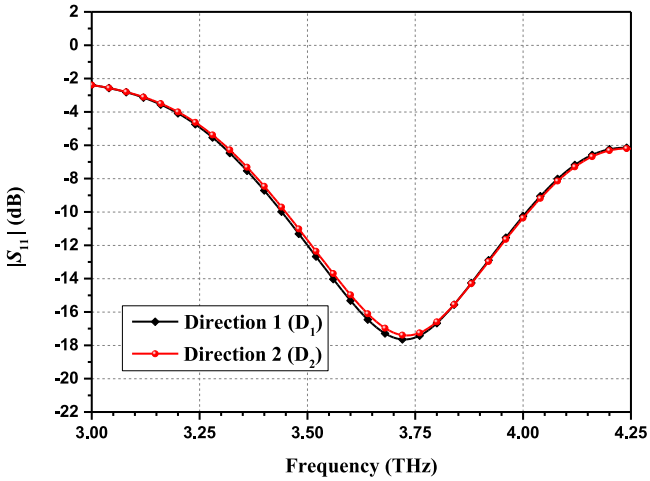

FIG. 4. Simulated reflection coefficients $|S_{11}|$ for the two-beam reconfigurable Yagi-Uda antenna for D_1 and D_2.

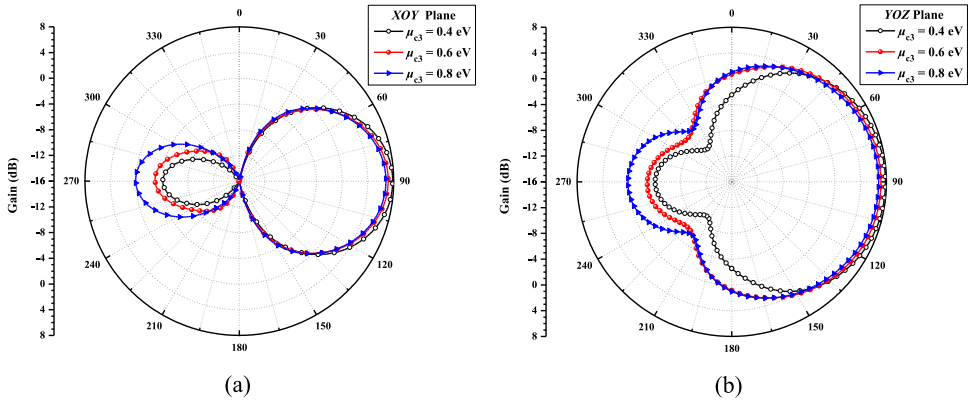

FIG. 5. Simulated radiation patterns of the proposed two-beam reconfigurable Yagi-Uda antenna with different chemical potentials at 3.73 THz for D_2: (a) *XOY* Plane, and (b) *YOZ* Plane.

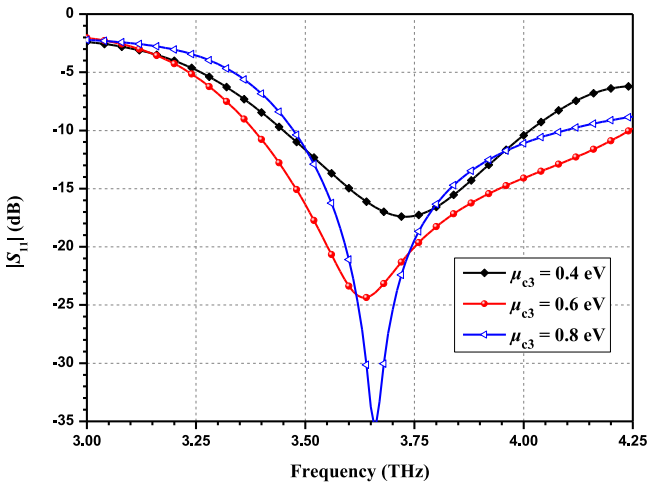

FIG. 6. Simulated reflection coefficients $|S_{11}|$ of the proposed two-beam reconfigurable Yagi-Uda antenna for three different chemical potentials μ_{c3} for D_2.

TABLE II. The accurate values of the chemical potentials for both D_1 and D_2 in the proposed two-beam reconfigurable Yagi-Uda antenna.

Directions	μ_{c1} (eV)	μ_{c2} (eV)	μ_{c3} (eV)
Direction 1(D_1)	0.4	0.4	0
Direction 2(D_2)	0.4	0	0.4

The front-to-back ratios as depicted in Figures 7(b) and 7(c) show small change within a range of 10.1 dB to 11.9 dB for τ varies from 0.2 ps to 1.0 ps, which can be ignored. Obviously, in the range of 0.4 to 1.0 ps (the considerable range in our paper), this kind of effects from the electron relaxation time τ is minimal and can be neglected.

III. THE DESIGN OF THE FOUR-BEAM RECONFIGURABLE YAGI-UDA ANTENNA

The layout structure and three-dimensional view of the four-beam reconfigurable Yagi-Uda antenna are shown in Figures 8(a) and 8(b). It consists of two orthogonal driven dipoles, four parasitic strips, and four parasitic rectangular loops. The values of chemical potentials μ_{c5} and μ_{c6} surrounding two dipoles determine which one will work. Adjusting the chemical potentials applied to the

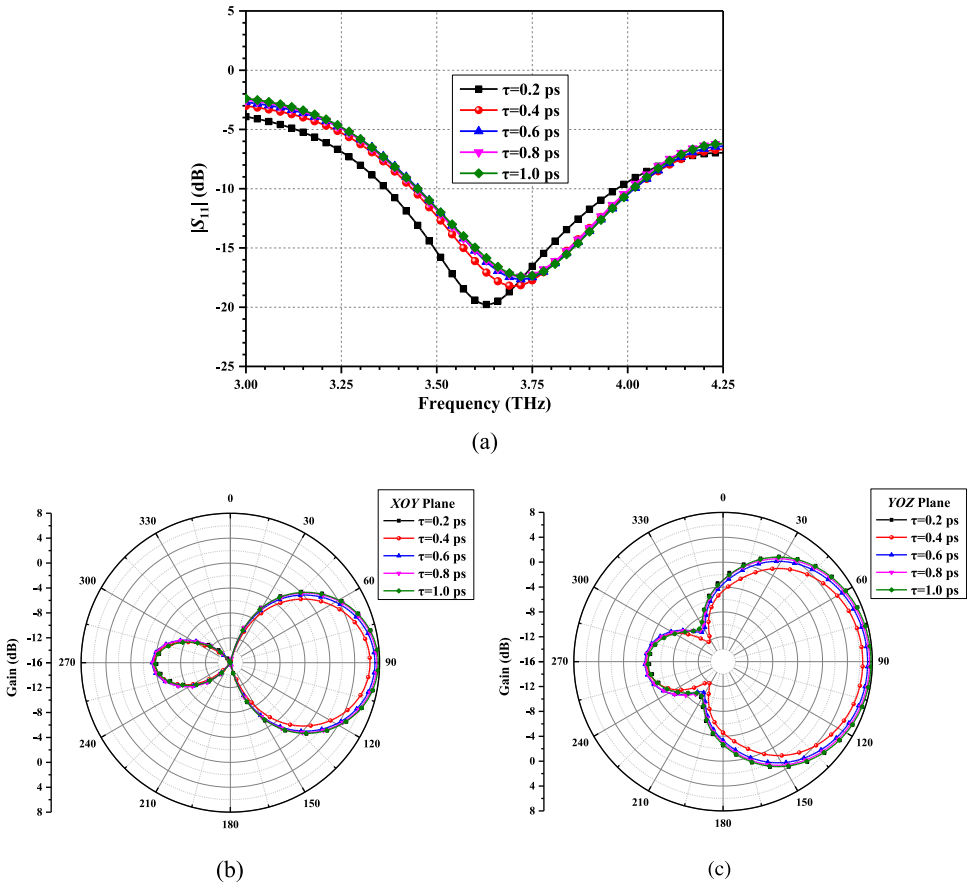

FIG. 7. The effect of the electron relaxation time τ on scattering parameters and radiation patterns at *XOY* Plane and *YOZ* Plane of the two-beam reconfigurable Yagi-Uda antenna for D_2: (a) The curves of $|S_{11}|$ with variable electron relaxation time τ when the chemical potentials μ_{c1} and μ_{c2} are set to 0.4 eV and μ_{c3} is 0 eV, and simulated radiation patterns of *XOY* Plane (b) and *YOZ* Plane (c) at 3.73 THz when the electron relaxation time τ changes from 0.2 ps to 1.0 ps.

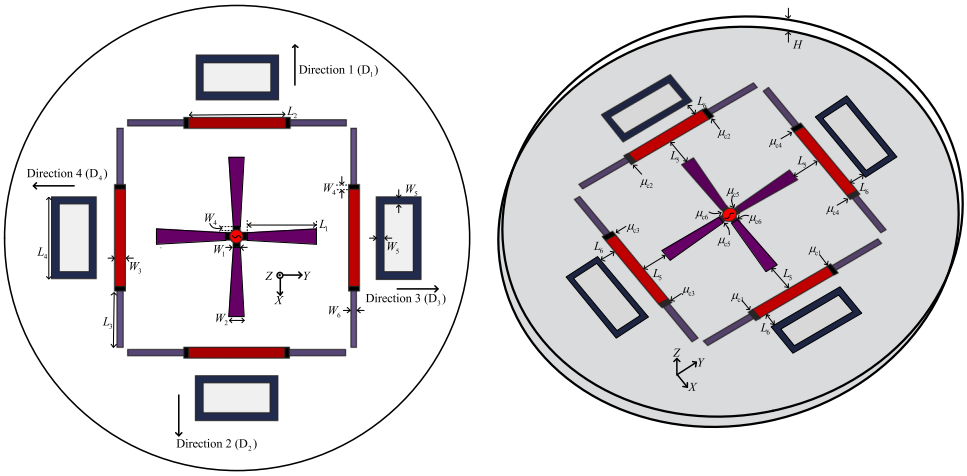

FIG. 8. Configuration of the four-beam reconfigurable Yagi-Uda antenna and parameter definitions: (a) top view, and (b) three-dimensional view.

graphene stubs in four parasitic strips will determine whether the parasitic strips act as directors or reflectors.

After careful simulation, a typical example for four-beam reconfigurable Yagi-Uda antennas is obtained. The final dimensions are tabulated in TABLE III. The five cross profiles and one three-dimensional radiation patterns of this proposed four-beam reconfigurable Yagi-Uda antenna at 1.88 THz are plotted in Figures 9(a)-9(c). It is very obvious and clear that four radiation patterns with different beams but similar shapes can be achieved in this proposed Yagi-Uda antenna. The parasitic strips, with two special chemical potentials of 3 eV and 0 eV, are capacitive and inductive and will act reflectors and directors, respectively.

When the Y-direction driven dipole is conductible (μ_{c5} = 3 eV and μ_{c6} = 0 eV), and the +X direction's chemical potential of the graphene in the parasitic strip μ_{c1} = 3 eV (μ_{c2} = 0 eV, μ_{c3} = 0 eV, and μ_{c4} = 0 eV), the proposed antenna has an end-fire radiation pattern in the –X direction (D_1). Similarly, when the chemical potential of the graphene in the -X direction μ_{c2} = 3 eV (μ_{c1} = 0 eV, μ_{c3} = 0 eV, and μ_{c4} = 0 eV), the proposed antenna has an end-fire radiation pattern in the +X direction (D_2). Based on the same operation, the proposed antenna can possess other two different beam patterns in +Y and -Y directions, namely, D_3 and D_4. The simulated results show that the peak gain of the proposed four-beam reconfigurable Yagi-Uda antenna is about 6.4 dB and its front-to-back ratio is about 12 dB. In addition, Figure 10 shows that the proposed antenna has stable reflection-coefficient performance although four main beams in reconfigurable cases point to four totally different directions, and the 10-dB impedance bandwidth is about 10 %. In order to further clarify the values of six chemical potentials for four directions (D_1, D_2, D_3, and D_4), TABLE IV lists the corresponding values of these six chemical potentials in the proposed antenna with four reconfigurable beams.

TABLE III. The geometrical parameters of the proposed four-beam reconfigurable Yagi-Uda antenna.

Parameters	Value (μm)	Parameters	Value (μm)	Parameters	Value (μm)
W_1	2	W_2	6	W_3	3.5
W_4	1	W_5	1.8	W_6	2
L_1	22	L_2	31	L_3	15.5
L_4	28	L_5	6.3	L_6	4.4

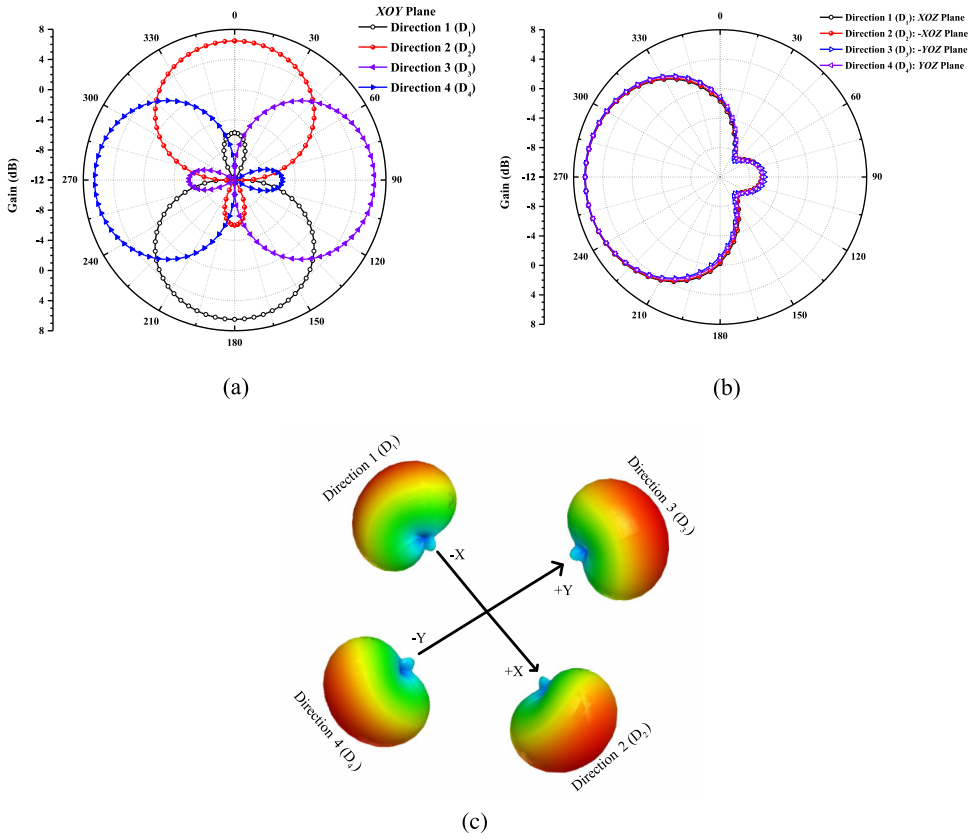

FIG. 9. Simulated radiation patterns of the proposed Yagi-Uda antenna with four reconfigurable beams at 1.88 THz: (a) *XOY* Plane, (b) four different Planes cutting along the Z direction, and (c) three-dimensional radiation patterns for D_1, D_2, D_3, and D_4.

Different from the previous two-beam reconfigurable Yagi-Uda antenna, four parasitic rectangular loops have been added in this four-beam reconfigurable Yagi-Uda antenna. As shown in Figure 11(a), the resonance frequency points of reflection coefficients $|S_{11}|$ will almost keep the same no matter whether the four rectangular loops are added or not. However, the front-to-back

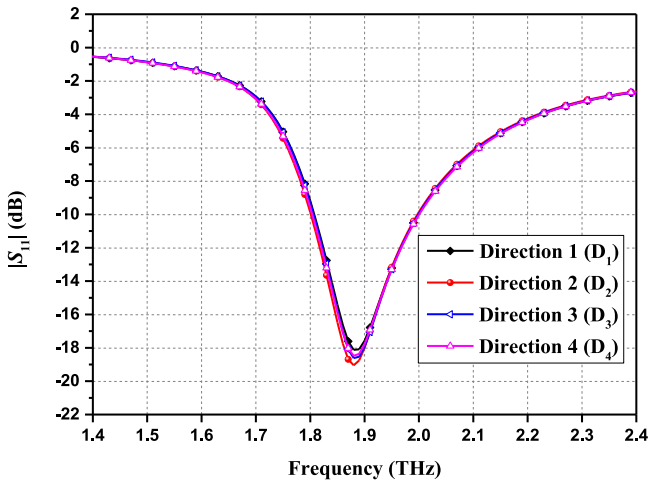

FIG. 10. Simulated reflection coefficients $|S_{11}|$ versus frequency for the proposed Yagi-Uda antenna with four reconfigurable beams operating at four different directions (D_1, D_2, D_3, and D_4).

TABLE IV. The values of the chemical potentials for D_1, D_2, D_3, and D_4 in the proposed four-beam reconfigurable Yagi-Uda antenna.

Parameters	Direction 1(D_1)	Direction 2(D_2)	Direction 3(D_3)	Direction 4(D_4)
μ_{c1} (eV)	3	0	0	0
μ_{c2} (eV)	0	3	0	0
μ_{c3} (eV)	0	0	3	0
μ_{c4} (eV)	0	0	0	3
μ_{c5} (eV)	3	3	0	0
μ_{c6} (eV)	0	0	3	3

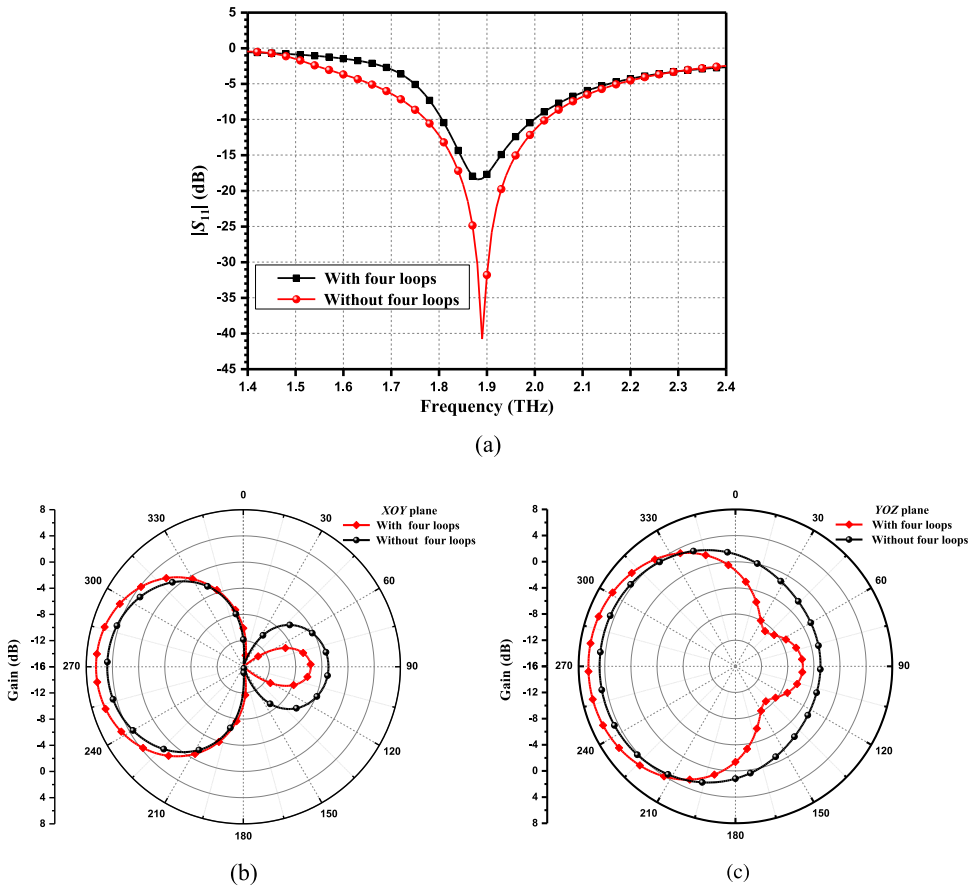

FIG. 11. Simulated results of the proposed four-beam reconfigurable Yagi-Uda antenna with or without four loop directors at 1.88 THz for D_4: (a) the reflection coefficients $|S_{11}|$, (b) the radiation pattern in *XOY* Plane, and (c) the radiation pattern in *YOZ* Plane.

ratios of this four-beam reconfigurable antenna at 1.88 THz are enhanced obviously from 7.7 dB to 12 dB in *XOY* Plane and *YOZ* Plane in Figure 11(b) and 11(c). Therefore, four parasitic rectangular loops behave as directors for enhancing the directivity of the proposed four-beam reconfigurable Yagi-Uda antenna. Similarly, the rectangular loops would also improve the front-to-back radio for the two-beam pattern reconfigurable Yagi-Uda antenna.[36]

IV. CONCLUSION

A kind of Yagi-Uda antenna based on graphene with radiation pattern reconfigurable function has been proposed in this article. The dynamic conductivity of the graphene, implanted in driven

dipole antenna and parasitic elements, which can be tuned by changing the chemical potential, allows the proposed antennas to change the radiation beam into two or four different directions. Due to the complex conductivity of the graphene, the parasitic strips can act as directors (reflectors) when they are inductive (capacitive). The function of the parasitic strips can be easily altered between directors and reflectors by simply changing the chemical potentials applied to the graphene. Excellent unidirectional symmetrical radiation patterns with the front-to-back ratio of 11.9 dB are achieved by choosing the suitable chemical potentials for the proposed two-beam reconfigurable Yagi-Uda antenna. The peak gain is about 7.8 dB and the 10-dB impedance bandwidth is about 15%. In the proposed four-beam reconfigurable Yagi-Uda antenna, the simulated results show that it has stable reflection-coefficient performance although four main beams in reconfigurable cases point to four totally different directions. The corresponding peak gain, front-to-back ratio, and 10-dB impedance bandwidth are about 6.4 dB, 12 dB, and 10%, respectively. It can be expected that this proposed design idea in this article possesses high potential for beam scanning in terahertz and mid-infrared plasmonic devices and systems, owing to the reconfiguration capabilities of the graphene and the end-fire characteristics of the Yagi-Uda antennas.

ACKNOWLEDGMENTS

This work was supported by National Basic Research Program of China (973 Program) (No. 2014CB339900), and National Natural Science Foundations of China (No. 61422103, No. 61327806, and No. 61201027).

[1] P. Russer and N. Fichtner, IEEE Microwave Magazine **11**(3), 119-135 (2010) 11256531.
[2] X. Hu, Master thesis, University of Toronto, Toronto, 2013.
[3] D. C. Serrano, Master thesis, Technical University of Cartagena, Cartagena, 2015.
[4] M. Dragoman, A. A. Muller, D. Dragoman, F. Coccetti, and R. Plana, Journal of Applied Physics **107**, 1-3 (2010) 104313.
[5] X. J. Huang, T. Leng, M. J. Zhu, X. Zhang, J. C. Chen, K. H. Chang, M. Aqeeli, A. Geim, K. Novoselov, and Z. R. Hu, Science Reports **5**, 1-8 (2015), 18298.
[6] E. Carrasco and J. Perruisseau-Carrier, IEEE Antennas and Wireless Propagation Letters **12**, 253-256 (2013).
[7] J. Nakabayashi, D. Yamamoto, and S. Kurihara, Physical Review Letters **102**, 11248-11256 (2009) 066803.
[8] D. Correas-Serrano, J. S. Gomez-Diaz, J. Perruisseau-Carrier, and A. Álvarez-Melcón, IEEE Transactions on Nanotechnology **13**(6), 1145-1153 (2014).
[9] F. Rana, IEEE Transactions on Nanotechnology **7**(1), 91-99 (2008).
[10] J. Tao, X. C. Yu, B. Hu, A. Dubrovkin, and Q. J. Wang, Optics Letters **39**(2), 271-274 (2014).
[11] Y. P. Zhang, T. T. Li, Q. Chen, H. Y. Zhang, J. O'Hara, E. Abele, A. Taylor, H.-T. Chen, and A. Azad, Science Reports **5**, 1-8 (2015), 18463.
[12] S. O. Yurchenko, K. A. Komarov, and V. I. Pustovoit, AIP Advances **5**, 1-12 (2015), 057144.
[13] X. -S. Yang, B. -Z. Wang, W. X. Wu, and S. Q. Xiao, IEEE Antennas and Wireless Propagation Letters **6**, 168-171 (2007).
[14] J. -W. Baik, S. Pyo, T. -H. Lee, and Y. -S. Kim, ETRI Journal **31**(3), 318-320 (2009).
[15] C. Kittiyanpunya and M. Krairiksh, IEEE Transactions on Antennas and Propagation **61**(12), 6210-6214 (2013).
[16] T. Zhang, S. -Y. Yao, and Y. Wang, IEEE Antennas and Wireless Propagation Letters **14**, 183-186 (2015).
[17] Z. Xu, X. D. Dong, and J. Bornemann, IEEE Transactions on Terahertz Science and Technology **4**(5), 609-617 (2014).
[18] M. Esquius-Morote, J. S. Gómez-Díaz, and J. Perruisseau-Carrier, IEEE Transactions on Terahertz Science and Technology **4**(1), 116-122 (2014).
[19] X. -C. Wang, W. -S. Zhao, J. Hu, and W. -Y. Yin, IEEE Transactions on Nanotechnology **14**(1), 62-69 (2015).
[20] A. H. Radwan, M. D'Amico, and G. G. Gentili, in *Antennas and Propagation Conference (LAPC)* (Loughborough, 2014), pp. 671-675.
[21] H. -Q. Xia, Q. -X. Pan, J. Hu, and W. -Y. Yin, IEEE International Symposium on Antennas and Propagation & USNC/URSI National Ratio Science Meeting (2015) pp. 1462-1463.
[22] P. Nayeri, F. Yang, and A. Z. Elsherbeni, IEEE Antennas and Propagation Magazine **57**(4), 32-47 (2015).
[23] M. Dragoman, D. Neculoiu, A. -C. Bunea, G. Deligeorgis, M. Aldrigo, D. Vasilache, A. Dinescu, G. Konstantinidis, D. Mencarelli, L. Pierantoni, and M. Modreanu, Applied Physics Letters **106**, 1-5 (2015) 153101.
[24] T. Zhou, Z. Q. Cheng, H. F. Zhang, M. L. Berre, L. Militaru, and F. Calmon, Microwave and Optical Technology Letters **56**(8), 1792-1794 (2014).
[25] M. Tamagnone, J. S. Gomez Diaz, J. Mosig, and J. Perruisseau-Carrier, in *IEEE MTT-S International Microwave Symposium Digest* (2013), pp. 1-3.
[26] D. Puccinelli and M. Haenggi, IEEE Circuits and Systems Magazine **3**(3), 19-29 (2005).
[27] I. E. Lee, Z. Ghassemlooy, W. P. Ng, V. Gourdel, M. A. Khalighi, S. Zvanovec, and M. Uysal, in *9th IEEE/IET International Symposium on Communication Systems, Networks and Digital Signal Processing (CSNDSP)* (Manchester, UK, 2014), pp. 368-373.
[28] X. Cheng, Y. Yao, S.-W. Qu, Y. Wu, J. Yu, and X. Chen, Electronics Letters **52**(7), 494-496 (2016).
[29] M. Tamagnone, J. S. G. Diaz, J. Mosig, and J. Perruisseau-Carrier, in *2013 IEEE MTT-S International Microwave Symposium Digest*, MWSYM.2013.6697756:1-3 (2013).

[30] L. Wang, I. Meric, P. Y. Huang, Q. Gao, Y. Gao, H. Tran, T. Taniguchi, K. Watanabe, L. M. Campos, D. A. Muller, J. Guo, P. Kim, J. Hone, K. L. Shepard, and C. R. Dean, Science **342**(6158), 614-617 (2013).
[31] V. P. Gusynin, S. G. Sharapov, and J. P. Carbotte, Journal of Physics **19**, 1-25 (2007) 026222.
[32] G. W. Hanson, IEEE Transactions on Antennas and Propagation **3**, 747-747 (2008).
[33] G. W. Hanson, Journal of Applied Physics **103**, 064302 (2008).
[34] D. Correas-Serrano, J. S. Gomez-Diaz, A. Alù, and A. Álvarez Melcón, IEEE Transactions on Terahertz Science and Technology **5**(6), 951-960 (2015).
[35] Y. Luo and Q.-X. Chu, IEEE Antennas and Wireless Propagation Letters **15**, 564-547 (2016).
[36] J. Wu, Z. Zhao, Z. Nie, and Q.-H. Liu, IEEE IEEE Transactions on Antennas and Propagation **63**(4), 1832-1837 (2015).